VIII. STATISTICAL COMMUNICATION THEORY

Prof. Y. W. Lee
A. G. Bose
J. Y. Hayase
K. L. Jordan, Jr.
C. S. Lorens
A. H. Nuttall
K. H. Powers
J. Tierney
R. E. Wernikoff
H. E. White

A. A THEORY OF NONLINEAR SYSTEMS

The present study has been completed. It was submitted as a thesis in partial fulfillment of the requirements for the degree of Doctor of Science, Department of Electrical Engineering, M.I.T., June 1956, and will also be presented in Technical Report 309.

A. G. Bose

B. A UNIFIED THEORY OF INFORMATION

This work, which was submitted as a thesis in partial fulfillment of the requirements for the degree of Doctor of Science, Department of Electrical Engineering, M.I.T., June 1956, will be published as Technical Report 311.

K. H. Powers

C. OUTLINE OF LEBESGUE THEORY

This paper is a heuristic introduction to the theory of measure and integration (see abstract in the Quarterly Progress Report of Jan. 15, 1956, p. 91). A preliminary hectographed edition was published on March 8, 1956; the final version, including some slight revisions, will be published as Technical Report 310.

R. E. Wernikoff

D. STATISTICAL APPLICATION OF FLOW GRAPHS – MEAN OCCURRENCE OF A MARKOV STATE

Markov Systems represent an ideal application of flow-graph formulation and reduction (1). One of the properties that is conveniently formulated and solved is that of the mean occurrence of a transient Markov state.

Flow-graph formulation corresponds exactly to the descriptive Markov graph which represents the system. With this convenient formulation property, the mean occurrence of the various Markov states are obtained directly from the Markov graph with flow-graph techniques.

1. Mean Occurrence

In a transient Markov system each transient state s_k ($k = 1, \ldots, m$) will occur, on the average, a particular number of times. Essentially, this number is the mean occurrence of the state s_k. It is dependent upon the state s_j in which the transient starts.

In order to show how flow graphs aid in calculating the mean occurrence, consider an ensemble of transient experiments that start in state s_j.

The common statistical characteristic function is used to indicate an occurrence of the state $s_k\left(\xi^n_{jk_r} = 1\right)$ or a nonoccurrence $\left(\xi^n_{jk_r} = 0\right)$ on the n^{th} move in the r^{th} experiment. In each experiment, the number of occurrences of the particular state s_k is given by

$$O_r = \sum_{n=0}^{\infty} \xi^n_{jk_r} \tag{1}$$

This summation amounts to "counting" the number of occurrences. The mean occurrence is then

$$O_{jk} = \lim_{R \to \infty} \frac{1}{R} \sum_{r=1}^{R} O_r = \lim_{R \to \infty} \frac{1}{R} \sum_{r=1}^{R} \sum_{n=0}^{\infty} \xi^n_{jk_r} \tag{2}$$

But reversing the order of summations gives the result

$$O_{jk} = \sum_{n=0}^{\infty} \lim_{R \to \infty} \frac{1}{R} \sum_{r=1}^{R} \xi^n_r = \sum_{n=0}^{\infty} p^n_{jk} \tag{3}$$

where p^n_{jk} is the transitional probability from s_j to s_k in exactly n moves.

Flow graphs provide a convenient method of computing this infinite sum directly from the Markov graph. By introducing the recurrence relation

$$p^o_{jk} = \delta_{jk} \qquad\qquad p^n_{jk} = \sum_{r=1}^{m} p^{n-1}_{jr}\, p_{rk} \tag{4}$$

into the derived definition of mean occurrence and changing the order of summation we obtain the relation

$$O_{jk} = \delta_{jk} + \sum_{r=1}^{m} O_{jr}\, p_{rk} \qquad\qquad k = 1, 2, \ldots, m \tag{5}$$

In flow-graph notation, this set of equations corresponds exactly to the transient part of the Markov diagram in which the variable O_{jk} is associated with the state s_k, and the starting state s_j is driven with a unit source.

Solution of the graph for the variable O_{jk} with flow-graph techniques then produces the mean occurrence of the state s_k for the system that started in the state s_j.

2. Example of Mean Occurrence

Consider the Markov system shown in Fig. VIII-1, in which the transient starts in state s_2. The flow graph for computing the mean occurrence of the various states is shown in Fig. VIII-2, in which the variable O_{jk} is associated with the state s_k. From Fig. VIII-2, the following quantities are computed.

$$O_{21} = \frac{.8}{1 - (.4)(.8) - (.2)(.8) - (.5)(.8)(.8)} = 4$$

$$O_{22} = \frac{1}{1 - (.4)(.8) - (.2)(.8) - (.5)(.8)(.8)} = 5$$

$$O_{23} = \frac{.2 + (.5)(.8)}{1 - (.4)(.8) - (.2)(.8) - (.5)(.8)(.8)} = 3$$

Normally, the original Markov diagram (Fig. VIII-1) is used as the flow graph for computing these mean occurrences of the various states.

This example could represent a holding pattern for landing aircraft at fields S_a or S_b or it could represent a piece of switch equipment hunting for another piece of equipment S_a or S_b.

Flow-graph formulation and reduction constitute convenient means of finding the mean occurrence of a transient Markov state.

C. S. Lorens

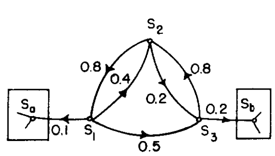

Fig. VIII-1. A Markov system.

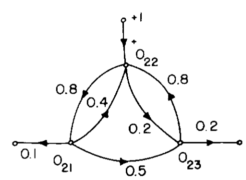

Fig. VIII-2. Flow graph of Fig. VIII-1 for computing mean occurrence.

References

1. C. S. Lorens, Quarterly Progress Report, Research Laboratory of Electronics, M.I.T., April 15, 1956, p. 60.

E. FORMULATION OF CASCADE CIRCUITS IN TERMS OF FLOW GRAPHS

A large number of electronic circuits are built in cascade. The mathematics of these systems should be a formulation that represents cascade systems. We are concerned with mathematical formulation in terms of flow graphs of elementary electrical elements in cascade. Individual flow graphs for the different electrical elements are presented in order to show how these graphs are cascaded in the same order in which the elements are cascaded in the physical circuit. An earlier report on this formulation will be found in reference 1; see references 2-6 for work on the reduction of the flow graph to the properties of the circuits.

1. Two Terminal-Pair Networks

Cascade circuits are usually made by cascading simple two terminal-pair networks. Two parallel formulations are used; one emphasizes current gain, the other voltage gain. Either formulation, or a combination of both, can be used.

The three-terminal electric network, shown in Fig. VIII-3, is conveniently represented mathematically by

$$\left.\begin{aligned} e_1 &= h_{11}\, i_1 + h_{12}\, e_2 \\ i_2 &= -h_{21}\, i_1 - h_{22}\, e_2 \end{aligned}\right\} \qquad (1a)$$

if we are interested in the current gain of the device, or by

$$\left.\begin{aligned} i_1 &= g_{11}\, e_1 - g_{12}\, i_2 \\ e_2 &= g_{21}\, e_1 - g_{22}\, i_2 \end{aligned}\right\} \qquad (1b)$$

if we are interested in the voltage gain of the device. The flow graphs for these formulations are shown in Fig. VIII-4a and b.

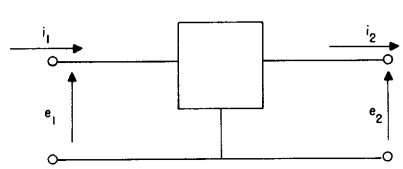

Fig. VIII-3. Two terminal-pair network.

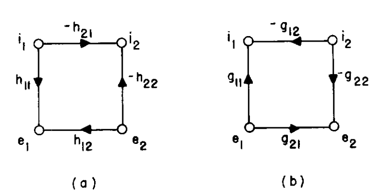

Fig. VIII-4. Flow graphs: (a) voltage gain; (b) current gain.

2. Cascading

The two terminal-pair flow-graph elements are cascaded in the same manner as the physical elements. The output of a current-gain element drives the input of another current-gain element. The same is true for voltage-gain elements.

The cascading of current-gain networks or voltage-gain networks, as in Fig. VIII-5, is accomplished on the basis of

$$\left.\begin{aligned} i_2 &= i_3 \\ e_2 &= e_3 \end{aligned}\right\} \tag{2}$$

The procedure involves connecting the flow-graph elements with lateral branches of +1 that have the same direction as the branches in the elements.

The advantage of this formulation is that the flow-graph element has the same characteristics as the electrical element and is cascaded in the same physical relation. For instance, the input impedance of the current-gain device is observed by looking into it on the left-hand side. In like manner, if we look into the representative flow graph on the left-hand side, we see the input impedance h_{11}. Another important characteristic of the current-gain device is the forward current gain h_{21}. In the flow graph this gain is represented by the forward-pointing arrow between the input and output currents.

By setting up the flow graphs in this manner, all of the currents can be made to appear on the upper level, and all of the voltages on the lower level. This is convenient from a dimensional standpoint because all of the branches pointing downward are impedances and all of the branches pointing upward are admittances. Lateral branches are dimensionless; in bilateral networks the branches are equal.

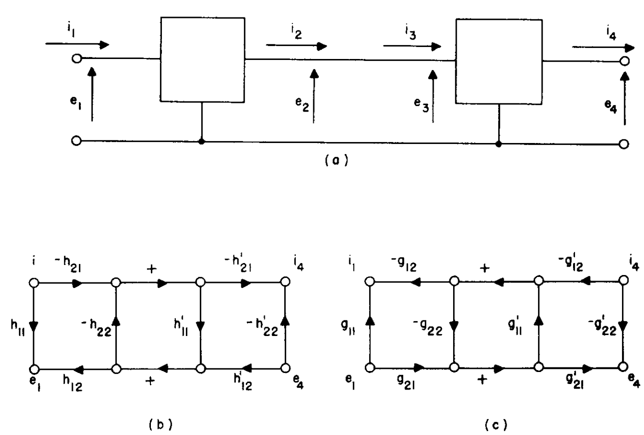

Fig. VIII-5. Flow graph: (a) cascading networks; (b) current gain; (c) voltage gain.

3. Mixed Cascading

In order to have a current-gain device cascade with a voltage-gain device, we have to perform an inversion at the output of the first device or at the input of the second device. There are a number of inversion methods. One method involves inverting the path and its coefficients and changing the sign of incoming branches (7).

The flow graph of a current-gain device cascaded with a voltage-gain device is represented either by Figs. VIII-6b or 6c. In Fig. VIII-6b, the output branch of the current-gain device is inverted; in Fig. VIII-6c, the input branch of the voltage-gain device is inverted.

4. Elementary Components

It is interesting to see what specific electrical elements look like in this flow-graph formulation. Figure VIII-7 shows the more common elements used in pure cascade networks. The current-gain representation is on the left-hand side; the voltage-gain representation is on the right-hand side. The gyrator is neither a current-gain nor voltage-gain device but a crossover from one to the other. The grounded cathode and cathode-follower vacuum-tube amplifiers are inherently voltage-gain devices so that no current-gain equivalent actually exists. However, they can be represented as voltage-to-current gain devices, as indicated in Fig. VIII-7.

The voltage-gain model for the transistor is not used in practice. It is included here only for completeness. Both grounded-base and grounded-emitter constants are shown for the transistor. The grounded-input transistor provides a method of going from one system to the other.

The most practical method of connecting devices in cascade is to have voltage

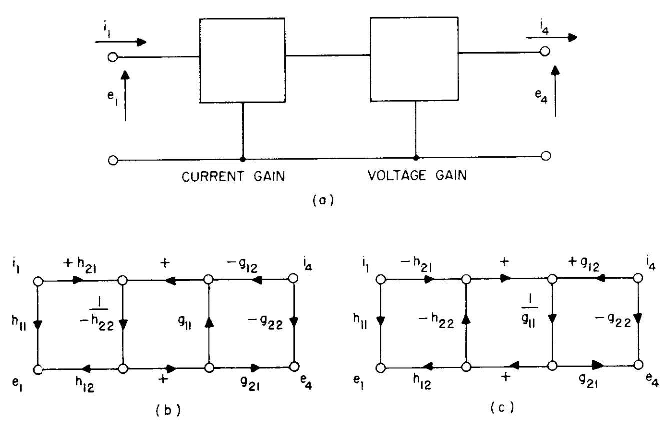

Fig. VIII-6. Flow graph: (a) mixed cascading; (b) current inversion; (c) voltage inversion.

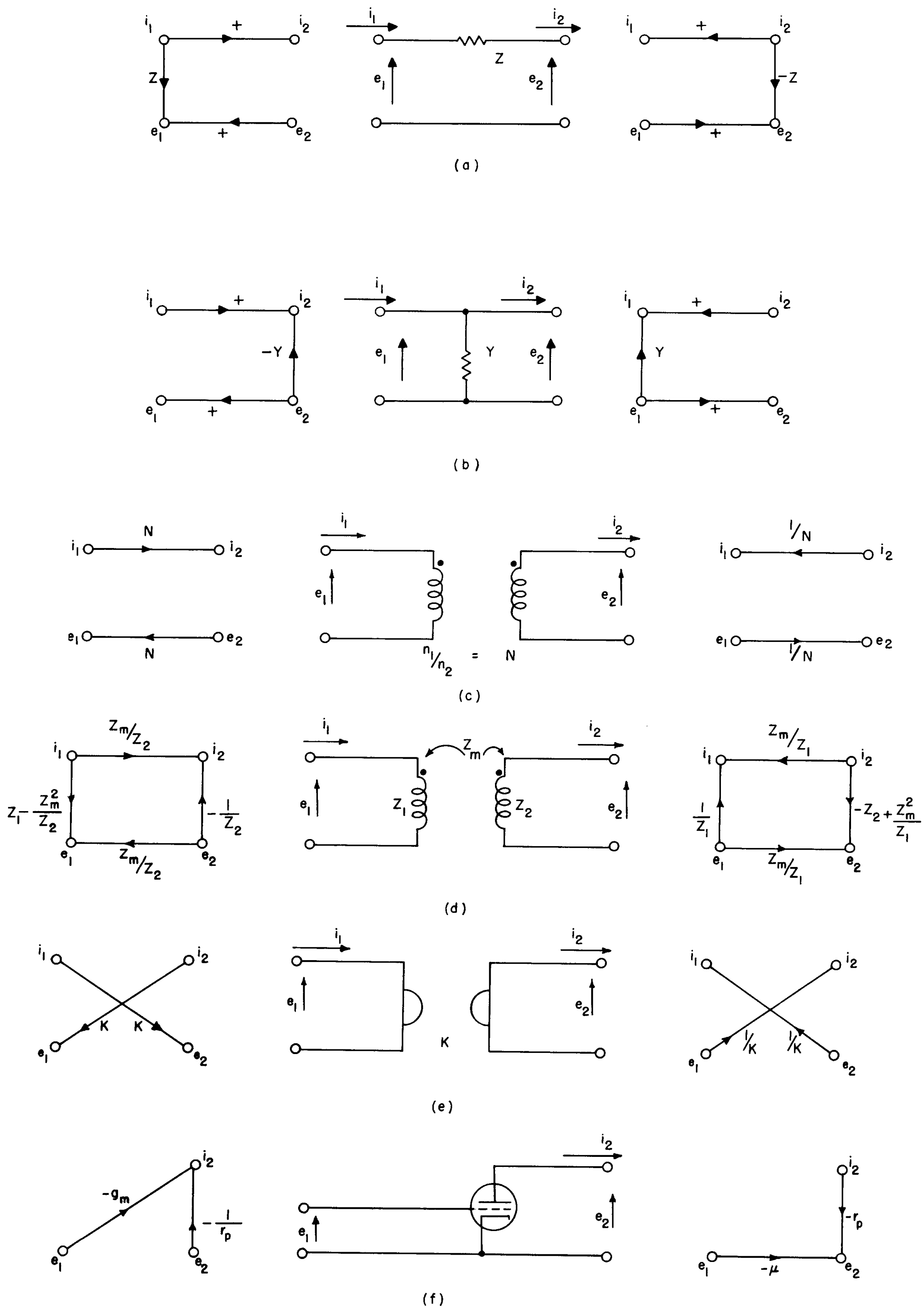

(continued on the following page)

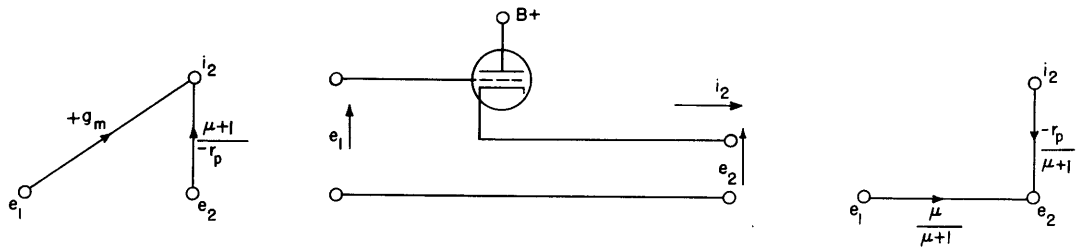

(g)

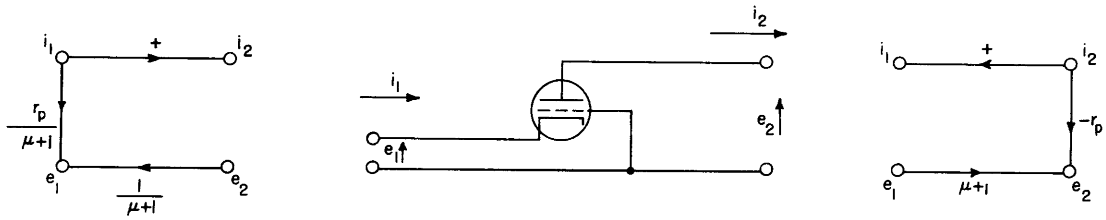

(h)

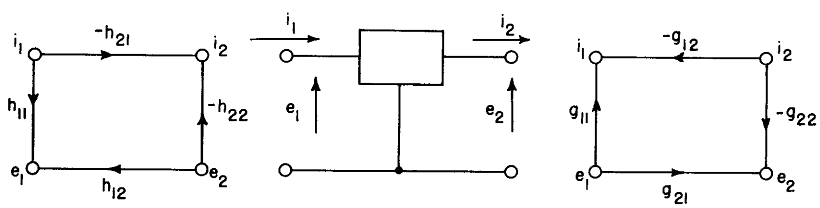

(i)

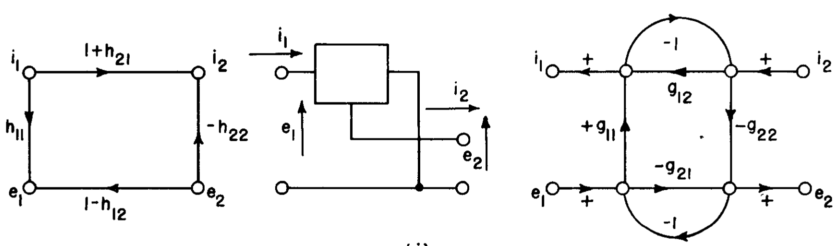

(j)

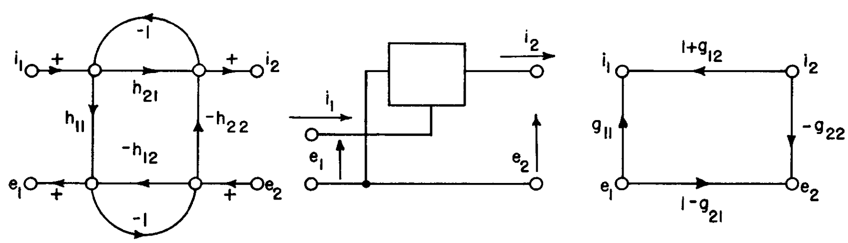

(k)

Fig. VIII-7. Elements of cascade networks: (a) series impedance; (b) shunt admittance; (c) ideal transformer; (d) physical transformer; (e) ideal gyrator; (f) grounded-cathode vacuum-tube amplifier; (g) cathode follower; (h) grounded-grid vacuum-tube amplifier; (i) grounded transistor amplifier; (j) grounded-output transistor amplifier; (k) grounded-input transistor amplifier.

circuits drive voltage circuits and current circuits drive current circuits. If the system contains both transistors and vacuum tubes, the crossover is usually made in the vacuum-tube unit, otherwise an inversion is necessary.

Termination of a current system is accomplished with a series impedance; termination of a voltage system is accomplished with a shunt admittance.

The importance of this formulation stems from the fact that networks are usually built in cascade. The ability to set up the mathematical formulation so that it carries along the intuitive feeling of cascade structure facilitates our understanding of the implications of the mathematics.

5. Examples

In order to illustrate these points, three examples are included. Note how the flow graph representing the physical circuit "strings out" in the same manner as the circuit.

The first example (Fig. VIII-8) shows two transistors embedded in an electrical ladder. The flow graph is set with current-gain elements by noting the physical position of the elements in the circuit.

The second example (Fig. VIII-9) shows the use of a vacuum-tube device driving a current device.

The third example (Fig. VIII-10) demonstrates the use of an inversion. The inversion is necessary in order to counteract the effect of the change-over of the gyrator from current to voltage gain. The input to the shunt-admittance model could not be inverted because the input impedance is zero.

C. S. Lorens

References

1. C. S. Lorens, Application of flow graphs to transistor circuits, General Electric Technical Information Series No. DF55ELP168, Dec. 20, 1955.
2. C. S. Lorens, Quarterly Progress Report, Research Laboratory of Electronics, M.I.T., Jan. 15, 1956, p. 97.
3. S. J. Mason, Sc. D. Thesis, Department of Electrical Engineering, M.I.T., 1952.
4. S. J. Mason, Proc. IRE 41, 1144 (Sept. 1953).
5. S. J. Mason, Technical Report 303, Research Laboratory of Electronics, M.I.T., July 20, 1955.
6. J. G. Truxal, Automatic Feedback Control Systems Synthesis (McGraw-Hill Book Company, New York, 1955) Chap. 2.
7. C. S. Lorens, Quarterly Progress Report, Research Laboratory of Electronics, M.I.T., April 15, 1956, p. 64, gives a more precise statement with proof and examples.

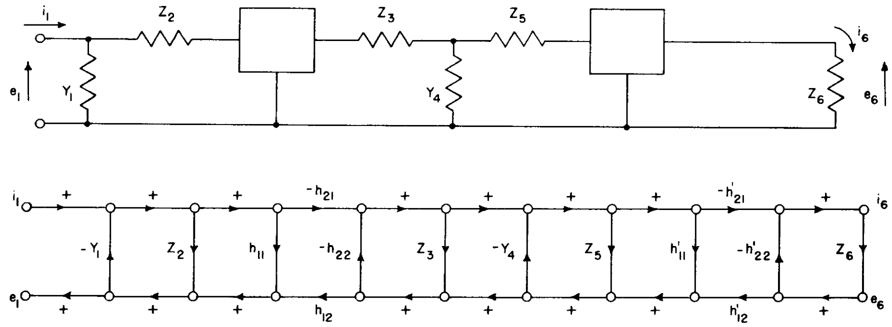

Fig. VIII-8. First example: transistors in an electrical ladder.

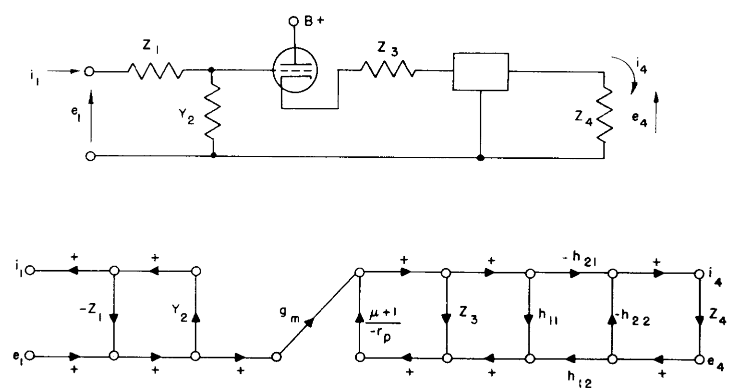

Fig. VIII-9. Second example: cathode-follower driving a transistor.

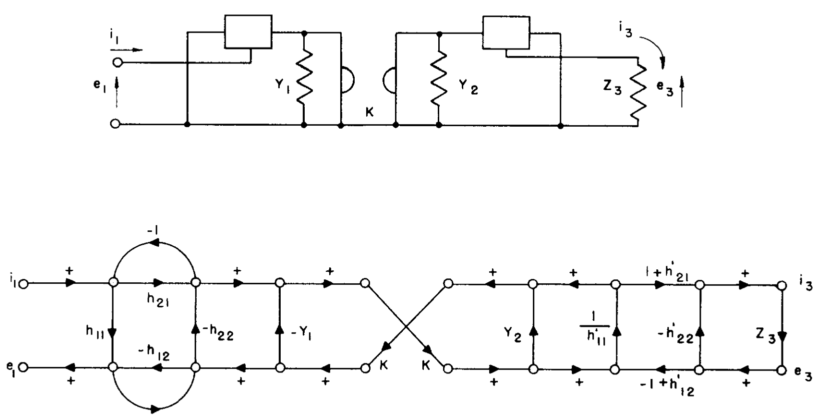

Fig. VIII-10. Third example: a necessary inversion.

F. PROPERTIES OF SECOND-ORDER CORRELATION FUNCTIONS

1. In the problem of field mapping by crosscorrelation, reported in the Quarterly Progress Report of October 15, 1954, page 66, the following relation was used without proof:

$$\overline{f(t)\, f(t+\tau_1)\, f(t+\tau_2)} \leq \overline{f^3(t)} \tag{1}$$

where f(t) is a non-negative function so chosen that the second-order autocorrelation function is finite for all τ_1 and τ_2.

This inequality can be obtained by applying Hölder's inequality (1) to the functions $f^3(t)$, $f^3(t+\tau_1)$ and $f^3(t+\tau_2)$ over the range $-T \leq t \leq T$.

$$\frac{1}{2T}\int_{-T}^{T} (f^3(t))^{1/3} \left(f^3(t+\tau_1)\right)^{1/3} \left(f^3(t+\tau_2)\right)^{1/3} dt$$

$$\leq \left[\frac{1}{2T}\int_{-T}^{T} f^3(t)\, dt\, \frac{1}{2T}\int_{-T}^{T} f^3(t+\tau_1)\, dt\, \frac{1}{2T}\int_{-T}^{T} f^3(t+\tau_2)\, dt\right]^{1/3}$$

$$= \left[\frac{1}{2T}\int_{-T}^{T} f^3(t)\, dt\, \frac{1}{2T}\int_{-T+\tau_1}^{T+\tau_1} f^3(t)\, dt\, \frac{1}{2T}\int_{-T+\tau_2}^{T+\tau_2} f^3(t)\, dt\right]^{1/3} \tag{2}$$

As T tends to infinity, Eq. 2 becomes

$$\lim_{T\to\infty} \frac{1}{2T}\int_{-T}^{T} f(t)\, f(t+\tau_1)\, f(t+\tau_2)\, dt$$

$$\leq \lim_{T\to\infty} \left[\frac{1}{2T}\int_{-T}^{T} f^3(t)\, dt\, \frac{1}{2T}\int_{-T+\tau_1}^{T+\tau_1} f^3(t)\, dt\, \frac{1}{2T}\int_{-T+\tau_2}^{T+\tau_2} f^3(t)\, dt\right]^{1/3} \tag{3}$$

But (see ref. 2),

$$\lim_{T\to\infty} \frac{1}{2T}\int_{-T}^{T} f^3(t)\, dt = \lim_{T\to\infty} \frac{1}{2T}\int_{-T+\tau_1}^{T+\tau_1} f^3(t)\, dt = \lim_{T\to\infty} \frac{1}{2T}\int_{-T+\tau_2}^{T+\tau_2} f^3(t)\, dt = \overline{f^3(t)} \tag{4}$$

so the right-hand side of Eq. 3 becomes $\overline{f^3(t)}$, and inequality 1 is obtained.

2. It was pointed out in the Quarterly Progress Report of October 15, 1955, page 49, that a significant difference between the first-order and second-order autocorrelation functions is that the former discards all the phase relation between the components of a periodic function, although the latter does not. To elaborate on this point, the first- and second-order autocorrelation functions of a trigonometric polynomial f(t) will be obtained.

$$f(t) = \sum_{k=1}^{N} A_k \cos(k\omega_o t + \theta_k) \tag{1}$$

where $T = \frac{2\pi}{\omega_o}$ is the period and θ_k is the phase angle of the k^{th} component. The first-order autocorrelation function of f(t) is

$$\phi(\tau) = \frac{1}{2} \sum_{k=1}^{N} A_k^2 \cos k\omega_o \tau \tag{2}$$

and the second-order autocorrelation function is

$$\begin{aligned}\phi(\tau_1, \tau_2) = \frac{1}{4} \Bigg[& \sum_{k=1}^{N} \sum_{\substack{m=1 \\ n=k+m}}^{N} \sum_{n=1}^{N} A_k A_m A_n \cos\left\{\omega_o(m\tau_1 - n\tau_2) + \theta_k + \theta_m - \theta_n\right\} \\ & + \sum_{k=1}^{N} \sum_{\substack{m=1 \\ n=m-k}}^{N} \sum_{n=1}^{N} A_k A_m A_n \cos\left\{\omega_o(m\tau_1 - n\tau_2) + \theta_m - \theta_k - \theta_n\right\} \\ & + \sum_{k=1}^{N} \sum_{\substack{m=1 \\ n=k-m}}^{N} \sum_{n=1}^{N} A_k A_m A_n \cos\left\{\omega_o(m\tau_1 + n\tau_2) + \theta_m - \theta_k + \theta_n\right\} \Bigg]\end{aligned} \tag{3}$$

In this expression, the sums are taken over values of k, m, and n that satisfy the relation shown below each of the triple summation signs.

Equation 3 shows that the phase angles of the n^{th}, k^{th}, and m^{th} harmonics enter the expression of $\phi(\tau_1, \tau_2)$ as $\theta_k + \theta_m - \theta_n$, $\theta_m - \theta_k - \theta_n$, and $\theta_m - \theta_k + \theta_n$, when the relation between n, m, and k is given by $n = k + m$, $n = m - k$, and $n = k - m$, respectively.

J. Y. Hayase

References

1. G. H. Hardy, J. E. Littlewood, and G. Pólya, Inequalities (Cambridge University Press, Ed. 2, 1952), p. 139.
2. N. Wiener, The Fourier Integral and Certain of Its Applications (Dover Publications, Inc., New York, 1953), p. 155.

G. THEORY OF NETWORK SYNTHESIS

[Editor's note: Under this heading we planned to present R. E. Wernikoff's translation of "Sobre la Sintesis de Sistemas Lineales para la Transmision sin Retraso, Retrasada y Prediccion Lineal de Señales," by M. V. Cerrillo, which was published in Revista Mexicana de Fisica (vol. 4, No. 2, 1955). The paper, which gives an application of the theory contained in Technical Report 270, by Dr. Cerrillo, "On Basic Existence Theorems. Part V. Window Function Distribution and the Theory of Signal Transmission" (to be published), is basic to work being done by the statistical communication theory group and other groups in the Laboratory, and is particularly appropriate in connection with Section VIII-H. Because of its length we regretfully postpone its publication until the Quarterly Progress Report of October 15, 1956.]

H. SOME RESULTS IN THE CERRILLO THEORY OF NETWORK SYNTHESIS

The impulse response of a linear, passive, two terminal-pair network will be called "singular" if it consists only of a finite number of impulses of finite area distributed over a finite time interval. Singular impulse responses have been studied by Dr. M. V. Cerrillo (1). The object of this report is to show how his results can be obtained from a different approach. First, we show why singular impulse responses are useful and interesting; then we derive the impulse areas appropriate to the problems of pure transmission, and delayed and advanced transmission. The technique used in arriving at these results will suggest natural directions in which the theory might be continued and generalized.

1. Equivalence of Smooth and Singular Impulse Responses

A linear system can be characterized completely in many different ways. In particular, the system can be specified completely by prescribing the unit impulse response, or its integral, the unit step response. Thus, if it can be shown that two networks have equal step responses, or that the step response of one approaches that of the other in the course of some suitable limit process, then, in the limit, the networks will give equal outputs when excited by equal inputs.

Consider the step response $A(t)$ shown in Fig. VIII-11, and the simple function $A_n(t)$

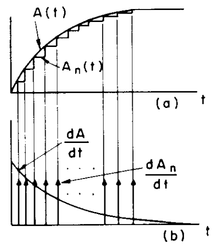

Fig. VIII-11. (a) Step responses. (b) Corresponding impulse responses.

which approximates A(t). The subscript n indicates the number of steps in $A_n(t)$. It can easily be shown that if A(t) is bounded and becomes substantially constant after a finite time (as is usually the case in physical systems) then it is possible to construct a sequence $\{A_n(t)\}$ of approximating functions that converges uniformly to A(t). When the unit step response is used to characterize a network, the output g(t) in terms of the input f(t) is given by (see, e.g., ref. 2, p. 153 et seq.)

$$g(t) = f(0)\, A(t) + \int_0^t \frac{df(\tau)}{d\tau} A(t-\tau)\, d\tau$$

$$= f(0) \left[\lim_{n\to\infty} A_n(t)\right] + \int_0^t \frac{df(\tau)}{d\tau} \left[\lim_{n\to\infty} A_n(t-\tau)\right] d\tau \tag{1}$$

Since $\{A_n\}$ converges to A uniformly, the limit and integral operations in Eq. 1 can be interchanged, yielding

$$g(t) = f(0) \left[\lim_{n\to\infty} A_n(t)\right] + \lim_{n\to\infty} \int_0^t \frac{df(\tau)}{d\tau} A_n(t-\tau)\, d\tau$$

$$= \lim_{n\to\infty} \left[f(0)\, A_n(t) + \int_0^t \frac{df(\tau)}{d\tau} A_n(t-\tau)\, d\tau\right] \tag{2}$$

The function inside the square brackets in Eq. 2 is the output of a network having as its step response the simple function $A_n(t)$. Thus, as in Eq. 2, we can represent the output g(t) of any network characterized by a suitable A(t) as the limit of the outputs of a sequence of networks whose step responses are simple functions. But the impulse response corresponding to the step response $A_n(t)$ is a singular response, since the (formal) derivative of a simple function is an array of impulses with each impulse corresponding to a step and having an area equal to the height of the step. Thus we have given, in effect, an informal proof of the theorem: The output of any linear network

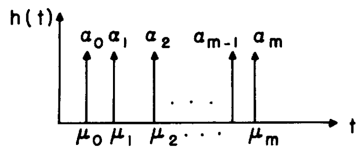

Fig. VIII-12. A singular impulse response.

whose step response A(t) meets the stated requirements (as most real networks do) can be represented as the limit of the outputs of a suitably chosen sequence of networks with singular impulse responses.

Since the sequence $\{A_n(t)\}$ converges to A(t), we can always find a finite number N which is sufficiently large so that the output of a network $A_N(t)$ approximates as closely as desired the output of the network A(t). If we now consider the impulse responses of the same networks, the statement simply becomes: The output of any network characterized by an impulse response which corresponds to a suitable A(t), can be approximated as closely as desired by the output of a network with a singular impulse response. In fact, it can even be shown that with some slight, and physically reasonable, additional restrictions on the continuity of A(t), the approximating singular responses can be so chosen that their impulses are equally spaced in time. The truth of these statements can be proved rigorously, and under even less stringent conditions than were assumed here, thus justifying our interest in singular impulse responses.

2. Transmission Problems

Consider the singular impulse response h(t) shown in Fig. VIII-12. The function h(t) consists of m + 1 impulses, the k^{th} impulse having an area a_k, which may be negative, and located at $t = \mu_k$. Let the total interval $\mu_m - \mu_o$ covered by the impulses be finite. We can express h(t) in the form

$$h(t) = \sum_{k=0}^{m} a_k\, \delta(t - \mu_k) \tag{3}$$

where $\delta(t)$ is the unit impulse at t = 0. If a network with impulse response h(t) is excited by an input f(t), its output g(t) is given by

$$g(t) = \int_{-\infty}^{t} f(\tau)\, h(t-\tau)\, d\tau = \int_{0}^{\infty} f(t-\tau)\, h(\tau)\, d\tau \tag{4}$$

If h(t) is the singular response given by Eq. 3, we obtain, substituting Eq. 3 in the second integral of Eq. 4,

$$g(t) = \int_{0}^{\infty} f(t-\tau) \sum_{k=0}^{m} a_k\, \delta(\tau - \mu_k)\, d\tau = \sum_{k=0}^{m} a_k\, f(t - \mu_k) \tag{5}$$

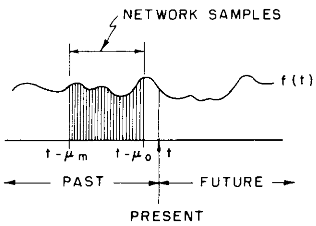

Fig. VIII-13. Segment of f(t) from which the network takes its sample values.

Equation 5 indicates the well-known fact that the present output of the network, g(t), is formed from a weighted sampling of the past (and possibly present) of the input function f(t). The situation is shown schematically in Fig. VIII-13, where μ_o may be zero. The network takes a finite number of samples of f(t) from the shaded region, and by combining these samples in some appropriate way, it forms an approximation to some desired function of f(t). We can describe this behavior by saying that the network is an interpolation operator on the past of the input. This point of view gives us a general procedure for determining, in Eq. 5, the coefficients a_k appropriate to the production of an output g(t) which is an approximation to some specified function of the input. (In fact, this point of view is more general than the one implied by Eq. 5. For example, since the information at the input to the network comes in a continuous wave, there is no a priori reason for limiting ourselves to the use of discrete samples of the wave, when we can, instead, employ interpolation techniques that make use of all the information contained in an interval of the past of the input. However, this approach to the problem will not be considered now.) Given the operation to be performed by the network, we choose an appropriate interpolation procedure to approximate the specified operation, and the procedure automatically gives us the required coefficients a_k. The appropriateness of an interpolation procedure is conditioned by, among other things, (a) its form (it must be a linear combination of sample values in order to have the same form as Eq. 5), (b) the magnitude of the error to which it leads in the given application, and (c) the ease with which it can be synthesized in network form.

As an example, suppose that we want to find a possible set of coefficients a_k appropriate to the following problems: (a) pure transmission, $[g(t) \approx f(t)]$; (b) delayed transmission, $[g(t) \approx f(t - T_o)]$; (c) advanced transmission, $[g(t) \approx f(t + T_o)]$. For this example, let us take our m + 1 sample points equally spaced, with spacing δ, and let $\mu_k = (k+1)\delta$, so that the network takes its samples in the interval $(t - \delta,\ t - (m+1)\delta)$. One of the simplest interpolation methods is the Lagrange method (ref. 3, p. 61), which amounts to nothing more than passing a polynomial $P_m(t)$ of order m through the m+1 sample points. Then, to obtain the value of the function for any given value of t, we simply determine the value of the polynomial at that value of t. Of course, in general, there is no necessary relation between the numbers f(t) and $P_m(t)$, but if the function has certain appropriate analytical properties, such as continuity, bounded derivatives, and so forth, we can expect that within certain ranges of values of t, $P_m(t)$ can serve as an estimate of $f(t)$. Error determination in interpolation and extrapolation, an important problem that is common to all methods, will not be considered here.

In forming the Lagrange polynomial, the writing is simplified if we take the origin of time at the present, and measure time positively in the direction of the past. With this meaning for the symbol t, the appropriate Lagrange polynomial is given by

$$P_m(t) = \sum_{k=0}^{m} f(\mu_k) \left[\frac{(t-\mu_o)(t-\mu_1)\dots(t-\mu_{k-1})(t-\mu_{k+1})\dots(t-\mu_m)}{(\mu_k-\mu_o)(\mu_k-\mu_1)\dots(\mu_k-\mu_{k-1})(\mu_k-\mu_{k+1})\dots(\mu_k-\mu_m)} \right] \qquad (6)$$

which can be condensed to

$$P_m(t) = \sum_{k=0}^{m} f(\mu_k) \prod_{j=0}^{m}{}' \left(\frac{t-\mu_j}{\mu_k-\mu_j} \right) \qquad (7)$$

where the prime on the product sign indicates that the factor $\left[(t-\mu_k)/(\mu_k-\mu_k)\right]$ is omitted.

If we want an approximation to $f(t)$ at $t = T$, we obtain it simply by determining $P_m(T)$. We want our network, which acts as an interpolation operator, to take the samples of $f(t)$ and combine them in such a way that the network output will be a determination of $P_m(T)$. In this way, the network will be using the samples of $f(t)$ to estimate, in the sense of Lagrange, the value of $f(t-T)$. To make the network output given by Eq. 5 resemble the polynomial in Eq. 7, let us evaluate Eq. 7 for $t = T$ and then change back to the original time scale. The factors in the product are left unchanged by the transformation of variables, and Eq. 7 becomes

$$P_m(T) = \sum_{k=0}^{m} f(t-\mu_k) \prod_{j=0}^{m}{}' \left(\frac{T-\mu_j}{\mu_k-\mu_j} \right) \qquad (8)$$

Comparing Eq. 8 with Eq. 5, we see that we shall achieve our purpose by setting

$$a_k = \prod_{j=0}^{m}{}' \left(\frac{T-\mu_j}{\mu_k-\mu_j} \right) \qquad (9)$$

Equation 9 is the solution of the problem, since it determines the network coefficients that realize our object. (In Eq. 9 it must be remembered that T is positive for delays, and that when $T = 0$, the output of the network is an approximation to the present of the input.)

If in Eq. 9 we use the relation $\mu_k = (k+1)\delta$, $(k = 0, 1, \dots, m)$ and measure T in units of δ by writing $T = \tau_o\delta$, the expression for the coefficients becomes

$$\alpha_k = \prod_{j=0}^{m}{}' \left(\frac{\tau_o - j - 1}{k - j} \right) \tag{10}$$

For $\tau_o > 0$, Eq. 10 gives the Cerrillo coefficients for delayed transmission.

For $\tau_o < 0$, Eq. 10 gives the Cerrillo coefficients for linear prediction.

For $\tau_o = 0$, Eq. 10 gives the Cerrillo coefficients for pure transmission. In this last case, Eq. 10 can be rewritten as

$$\alpha_k = (-1)^m \prod_{j=0}^{m}{}' \left(\frac{j+1}{k-j} \right) = (-1)^k \frac{(m+1)!}{(k+1)!\,(m-k)!} = (-1)^k \binom{m+1}{k+1} \tag{11}$$

where the last symbol represents the binomial coefficient.

For the purposes of this paper, the specific result (Eq. 10) is important only as an illustration of the application of the way of thinking in which networks (not necessarily linear) are regarded as interpolation operators. One of the most attractive features of this point of view is that it makes the very considerable body of results of numerical analysis directly available to the study of time-domain synthesis. In this direction lies an opportunity for the continuation and generalization of this work.

R. E. Wernikoff

References

1. M. V. Cerrillo, Sobre la Sintesis de Sistemas Lineales para la Transmision sin Retraso, Retrasada y Prediccion Lineal de Señales, Revista Mexicana de Fisica, 4, 2, 1955. (An English translation will be published in the Quarterly Progress Report, Oct. 15, 1956.)
2. L. B. Arguimbau, Vacuum-Tube Circuits (John Wiley and Sons, Inc., New York, 1948).
3. F. B. Hildebrand, Introduction to Numerical Analysis (McGraw-Hill Book Company, New York, 1956).

I. LEVEL SELECTOR TUBE

The first model of the level selector tube was described in the Quarterly Progress Report of January 15, 1956, page 107. In order to obtain a higher output strip current and to reduce the coupling between strips caused by secondary emission, a second model of the tube was constructed in the Barta Building tube laboratory. This model employs beryllium-copper output strips and a collector plate, as shown in Fig. VIII-14.

The secondary emission ratio, δ, of the beryllium-copper output strips was observed to be maximum in the region where the incident electron beam energy is 550 volts. A δ of approximately 4.2 was observed and a corresponding output strip

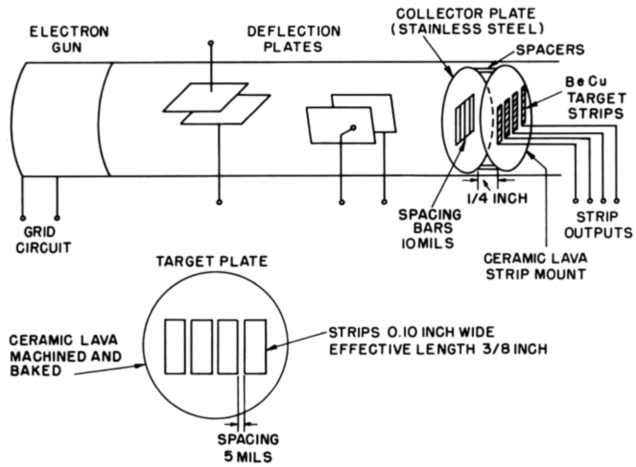

Fig. VIII-14. Diagram of selector tube (model 2).

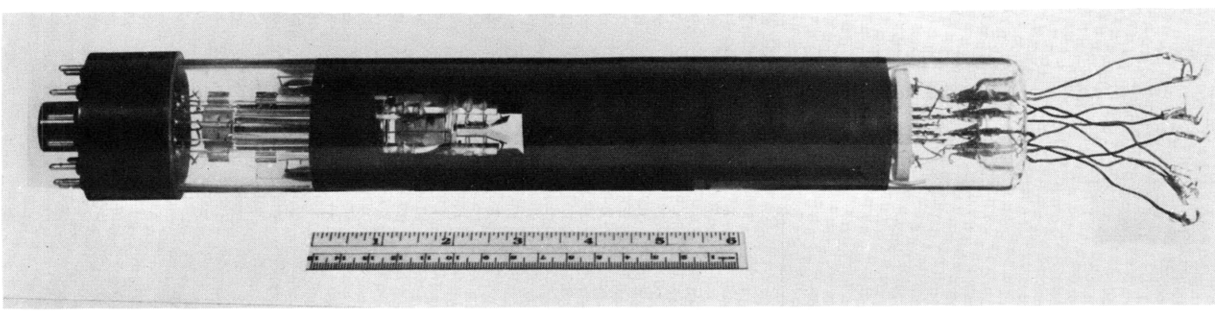

Fig. VIII-15. Level selector tube (model 2).

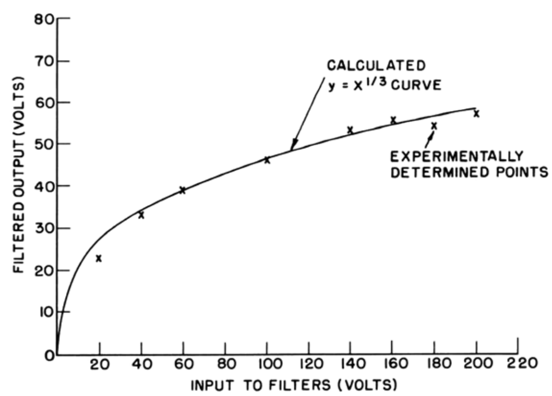

Fig. VIII-16. Filter for cube-law distorted signal.

current of 450 μamp was obtained.

In order to avoid high current densities on the surface of the beryllium-copper strips that could be detrimental, a sheet beam was formed. This was accomplished by taking advantage of the rectangular geometry of the deflection plates of a conventional electrostatic (5UP) cathode-ray gun to form the desired electron lens. The sheet beam was formed when a dc potential of 300 volts was applied between the deflection plates and the second anode. A photograph of the second model of the level selector tube is shown in Fig. VIII-15.

An application of the level selector tube for the determination of optimum no-storage nonlinear filters, in accordance with the theory discussed in the Quarterly Progress Report of October 15, 1955, page 43, is described in the Quarterly Progress Report of January 15, 1956, page 107. As a test of this application the optimum filter was determined for the case of the desired output equal to $x(t)$, with the signal to be filtered equal to $x^3(t)$. For convenience, $x(t)$ was taken to be a sine wave of audio frequency. The experimentally determined filter characteristic is shown in Fig. VIII-16, in which the solid line represents the desired cube root transfer characteristic.

A. G. Bose, J. Tierney